Food Control 85 (2018) 11–22

Contents lists available at ScienceDirect

Food Control

journal homepage: www.elsevier.com/locate/foodcont

Phenolic profiling of grapes, fermenting samples and wines using UV-Visible spectroscopy with chemometrics

Jose Luis Aleixandre-Tudo [a, b, *], Helene Nieuwoudt [c], Alejandro Olivieri [d], Jose Luis Aleixandre [a], Wessel du Toit [b]

[a] Departamento de Tecnologia de Alimentos, Universidad Politécnica de Valencia, Camino de Vera s/n, 46022 Valencia, Spain
[b] Department of Viticulture and Oenology, Stellenbosch University, Private Bag X1, Matieland 7602, South Africa
[c] Institute for Wine Biotechnology, Stellenbosch University, Private Bag X1, Matieland 7602, South Africa
[d] Departamento de Química Analítica, Facultad de Ciencias Bioquímicas y Farmaceuticas, Universidad Nacional de Rosario, Institutó de Química de Rosario (IQUIR-CONICET), Suipacha 531, Rosario S2002LRK, Argentina

ARTICLE INFO

Article history:
Received 3 August 2017
Received in revised form
12 September 2017
Accepted 13 September 2017
Available online 18 September 2017

Keywords:
UV-Visible spectroscopy
Chemometrics
Phenolic profiling
Grapes
Fermentation
Wines
Limit of detection

ABSTRACT

Phenolic compounds play and important role on colour, flavour and mouthfeel attributes of wines. The acquisition of information related to phenolic compounds during the winemaking process is therefore becoming a necessity. Ultraviolet-Visible (UV-Vis) spectroscopy appears as an affordable option to monitor phenolic composition and levels during winemaking. To investigate this, a large number of samples collected from industrial fermentations over two vintages as well as commercial wine samples, spanning a wide range of vintages, were analysed for phenolic compounds using high performance liquid chromatography (HPLC). Methyl cellulose precipitable (MCP) tannins, anthocyanins, total phenols and colour density were also analysed. Partial least-squares (PLS) calibration models, based on UV-VIS spectra and reference measurements, were constructed and their performance evaluated in terms of the residual predictive deviation values. The accuracy and robustness of the calibrations were further evaluated by a combined test on slope and intercept, interclass correlation coefficients and standard error of measurement. Limit of detection and limit of quantification of the PLS models were also reported and evaluated. Furthermore, PLS models for an additional data set including 130 grape samples was also investigated for MCP tannins, anthocyanins, total phenols and colour density measurements. Phenolic compounds were extracted following two different protocols, namely wine-like and homogenate methods.

1. Introduction

Phenolic compounds are bioactive substances that are widely distributed in plants and fruits and therefore also occur in some food products including wine (Teixeira, Eiras-Dias, Castellarin, & Gerós, 2013). Wine and grape derived phenolic compounds can be classified into non-flavonoids (hydroxycinnamates, hydroxybenzoates and stilbenes) and flavonoids (flavan-3-ols, flavonols and anthocyanins) (Garrido & Borges, 2013). Flavonoids and hydroxycinnamates are found in grapes and wines in high concentrations while the other non-flavonoid phenolics are found at lower levels (Teixeira et al., 2013). The importance of phenolic compounds resides in their role in colour, flavour and mouthfeel attributes of wines (Cheynier et al., 2006; Fulcrand, Dueñas, Salas, & Cheynier, 2006). Additionally, the health benefits of highly containing phenolic foods, such as wine, have been extensively documented (Aleixandre, Aleixandre-Tudó, Bolaños-Pizarro, & Aleixandre-Benavent, 2013). In combination with its antioxidant properties, protective effects against cardiovascular diseases (Chiva-blanch, Arranz, Lamuela-raventos, & Estruch, 2013), some cancers (Arranz et al., 2012, pp. 759–781) and neurodegenerative (Sun, Wang, Simonyi, & Sun, 2010, pp. 375–383) or inflammatory (Casas et al., 2012) diseases have been reported.

Grapegrowing and winemaking techniques can influence the levels of these compounds in the final product (Sacchi, Bisson, & Adams, 2005; Smith, Mcrae, & Bindon, 2015). The time-efficient quantification of phenolic compounds during the winemaking

* Corresponding author. Departamento de Tecnologia de Alimentos, Universidad Politécnica de Valencia, Camino de Vera s/n, 46022 Valencia, Spain.
E-mail address: joaltu@upvnet.upv.es (J.L. Aleixandre-Tudo).

https://doi.org/10.1016/j.foodcont.2017.09.014
0956-7135/

process is thus a necessity. Traditionally, ultraviolet-visible (UV-Vis) spectrophotometric based methods have been used for the analysis of the phenolic composition. UV-Visible methods are suitable for phenolic analysis because of the ability of these compounds to absorb UV (provide a protective effect in plants against UV radiation) and visible light (they are mostly coloured compounds) (Lorrain, Ky, Pechamat, & Teissedre, 2013). The intensity of the UV-Visible spectrum is attributed to the electronic transition of the π type orbitals, which depends on the number and the location of the OH, OCH_3 and glycoside groups of the different classes of polyphenols (Sanna et al., 2014). Intermolecular interactions and the conditions of the medium (pH, metals, SO_2) define the UV-Visible absorption of the phenolic pool (Hassane, Gierschner, Duroux, & Trouillas, 2012).

Spectrophotometric analyses of phenolic compounds are achieved through a number of protocols (Aleixandre-Tudo, Buica, Nieuwoudt, Aleixandre, & du Toit, 2017). These methods generally provide an estimation of the overall content of a specific subclass of phenolic compounds. A lack of specificity and reproducibility have been ascribed to these methodologies (Sun, Leandro, Ricardo da Silva, & Spranger, 1998). However, they have also been defined as reliable, simple, cost effective and fast procedures, which make them suitable for routine analytical practices (Aleixandre-Tudo et al., 2017; Harbertson & Spayd, 2006). On the other hand, high performance liquid chromatography (HPLC) analysis provide more accurate and precise quantification of phenolic compounds. In this case individual phenolics can be quantified thanks to the separation of the compounds after passing through the HPLC column (Boido, Alcalde-Eon, & Carrau, 2006). After elution, the phenolic compounds can be quantified at different wavelengths using a UV-Visible detector (Hassane et al., 2012). The main drawbacks of HPLC techniques are found in the necessity of skilled personnel, the costs involved in instrumentation and reagents and the lengthy analysis time.

The use of spectroscopy combined with chemometrics to quantify the levels of phenolic compounds in grapes and wines has been extensively reported (Cozzolino, 2015; Dambergs, Gishen, & Cozzolino, 2015; Ricci, Parpiniello, Laghi, Lambri, & Versari, 2013; Versari, Parpinello, & Laghi, 2012). The benefits claimed include reliability, rapidness, cost-effectiveness and simplicity (Dambergs et al., 2015; Gishen, Dambergs, & Cozzolino, 2005). Additionally, this multiparametric technique is highly suitable for on-line and in-line systems, which makes it appropriate for the control and monitoring of wine fermentation and aging processes (Cozzolino, 2015; Gishen et al., 2005). Although a large part of the published studies uses near and mid infrared spectroscopy, UV-Visible spectral information has been shown to also be useful for the quantification of wine phenolics (Aleixandre-Tudo, Nieuwoudt, Aleixandre, & Du Toit, 2015; Beaver & Harbertson, 2016; Dambergs, Mercurio, Kassara, Cozzolino, & Smith, 2012; García-Jares & Medina, 1995; Skogerson, Downey, Mazza, & Boulton, 2007). As mentioned, the ability of phenolics to absorb UV light and the fact that they are mostly coloured compounds make UV-Visible spectroscopy a suitable technique for this purpose.

A number of attempts to quantify phenolic content in fermenting samples and finished wines using UV or the combination of UV-Visible spectroscopy have been reported in the literature (Aleixandre-Tudo, Nieuwoudt, Aleixandre, & Toit, 2015; Beaver & Harbertson, 2016; Dambergs et al., 2012; García-Jares & Medina, 1995; Skogerson et al., 2007). The first research aiming to predict anthocyanin and tannin content using UV-Visible spectroscopy was reported by García-Jares and Medina (1995). Despite the limitations of the reference methods, due to non-specificity, and the limited sample set, the results showed the potential of UV-Visible spectroscopy to predict phenolic levels in wines. More recently, Dambergs et al. (2012) reported accurate multiple linear regression (MLR) and partial least-squares (PLS) regression calibrations for the quantification of methylcellulose precipitable tannins (MCP) using UV spectroscopy. A number of fermenting samples from small scale fermentation trials were included in the calibration set as well as in validation. In another study in finished wines, UV-Visible PLS prediction models for MCP and bovine serum albumin (BSA) tannins were also reported (Aleixandre-Tudo et al., 2015). Moreover, Skogerson et al. (2007) reported PLS models with varying level of accuracy, for commercial fermenting samples collected over one vintage for the Adam-Harbertson assay phenolic parameters (Harbertson, Picciotto, & Adams, 2003). An updated research investigating the effect of several factors on the accuracy of UV-Visible spectroscopy models to quantify the Adam-Harbertson phenolic parameters was recently reported (Beaver & Harbertson, 2016). The effect of wine dilution, pH stability and cultivar (Shiraz and Cabernet Sauvignon samples were included) on model performance was investigated (Beaver & Harbertson, 2016). The updated BSA assay protocol reported by Harbertson, Mireles, and Yu (2015) was in this case used as reference method. Again, prediction models with varying accuracy were reported.

Surprisingly, no references were found in the literature regarding attempts to provide calibration models for grape phenolic composition using UV-Visible spectroscopy. Several publications reported prediction models for grape phenolic analysis using infrared spectroscopy (Chen et al., 2015; Fernandes et al., 2011; Ferrer-Gallego, Hernández-Hierro, Rivas-Gonzalo, & Escribano-Bailón, 2011; Fragoso, Aceña, Guasch, Busto, & Mestres, 2011). Moreover, different methods for the extraction of phenolic compounds from the solid part of the berries with varying extraction conditions have been reported in the literature (Bindon et al., 2014; Iland, Ewart, Sitters, Markides, & Bruer, 2000). One of the most widely accepted methods relies on the phenolic extraction of blended or homogenized berries. Although strong correlations for colour and anthocyanins measurements in grape and wine data were reported (Bindon et al., 2014; du Toit & Visagie, 2012; Jensen, Werge, Egebo, & Meyer, 2008), moderate to weak correlations were observed between the tannin levels in grapes and those measured in the corresponding wines (du Toit & Visagie, 2012; Jensen et al., 2008). On the other hand, a method simulating the phenolic extraction that occurs during the fermentation process was recently reported by Bindon et al. (2014). Strong positive correlations for MCP tannin levels in Cabernet Sauvignon and Shiraz grapes and the wines made thereof were reported. The investigation of prediction models using UV-Vis spectroscopy in grapes extracts would thus provide scientists and winemakers with additional suitable techniques that might be used for the quantification and monitoring of phenolic composition during grape ripening as well as at harvest.

Taking into account that UV Visible spectroscopy is generally a more affordable and available technique for medium and small sized wineries (compared with infrared technology), the main aim of this research was thus to firstly investigate the suitability of UV-Visible spectroscopy for the determination of the phenolic profile of wine samples during fermentation as well as for finished wines. A total of 27 individual phenolic compounds were quantified from the HPLC analysis of a large number (569) of fermenting samples and wines. Moreover, conventional methods were used to measure MCP tannins, anthocyanins, total phenolics and wine colour density. PLS prediction models for HPLC and spectrophotometric analyses were built and validated. The second aim of the study corresponds to the investigation of PLS prediction models for the quantification of phenolic composition of grape berry extracts using two different extraction protocols.

2. Material and methods

2.1. Reagents and standards

Malvidin-3-glucoside chloride was purchased from Extrasynthese (Lyon, France). Phosphoric acid and caffeic acid were purchased from Fluka (Sigma-Aldrich Chemie, Steinheim, Germany). Acetonitrile was obtained from Merck (Darmstadt, Germany). Finally, gallic acid, catechin, *p*-coumaric acid, quercetin-3-glucoside and quercetin were obtained from Sigma-Aldrich Chemie, (Steinheim, Germany). The reagent used for the spectrophotometric analysis (methyl cellulose, ammonium sulphate, hydrochloric acid (HCl)) were also obtained from Sigma-Aldrich Chemie, (Steinheim, Germany).

2.2. Grape samples

One hundred and thirty batches of grapes were collected in 2016 from a variety of wine sub-regions within the Western Cape region in South Africa. The sample set was composed by a large number of cultivars namely: Cabernet Sauvignon (27), Cabernet Franc (2), Cinsault (3), Grenache (3), Malbec (5), Merlot (13), Mourvedre (2), Durif (2), Petit Verdot (6), Pinotage (15), Red Muscadel (1), Roobernet (1), Shiraz (46), Tannat (1) and Tempranillo (1) and two unknown samples. Two phenolic extraction protocols were performed and prediction models were built for four spectrophotometric determinations (MCP tannins (mg/g), anthocyanins (mg/g), total phenolics index and colour density).

2.3. Wine samples

Fermenting samples from different vinifications were collected in 2015 (n = 9) and 2016 (n = 4), from the commercial Welgevallen cellar (Stellenbosch, South Africa). The three main South African cultivars, namely Cabernet Sauvignon, Shiraz and Pinotage, together with a Grenache vinification were included in the sample set. Samples were collected on a daily basis for the first 15 days and every 3 days for a maximum period of two months from grape crushing. With the aim of including a large diversity of winemaking conditions, the selected vinifications included the following winemaking techniques: different yeast strains, cold maceration, tannin addition, extended maceration and malolactic fermentation in barrel. Additionally, the grape batches contained varying phenolic and sugar ripening levels. Fermentations took place in a variety of different fermenters from 3.000 to 10.000 L in size. Samples were filtered with a kitchen sieve and frozen until analysis. Before spectral collection or chemical analysis, samples were thawed at room temperature overnight and centrifuged at 3248*g* for 5 min (7366 Hermle centrifuge (Wehingen, Germany)). A total number of 391 fermenting samples were collected over the two vintages. In order to extend the prediction ability of the models, 178 finished wine samples that represented a wide range of cultivars (15) and vintages (2005–2016), as well as some blends, were also collected, analysed and included in the calibrations.

2.4. Extraction of phenolic compounds from grapes

The extraction of phenolic compounds from grape berries was performed following the protocols reported by Iland et al. (2000) and Bindon et al. (2014). For the homogenate method (Iland et al., 2000), a sub-sample of 50 berries was randomly selected and homogenized for 2 min using an Ultra-Turrax T25 high speed homogenizer (Janke & Kunkel GmbH & Co., Germany). Homogenates were frozen until analysis. Prior to analysis samples were allowed to thaw overnight. The extraction using the simulating wine-like conditions reported by Bindon et al. (2014) was performed as follows: 50 g of fresh grapes placed in a re-sealable zipper bag were gently crushed by hand. Crushed grape berries and juice were transferred to 250 mL dark glass bottles covered with foil. 15 mL of extraction solvent (40% ethanol (v/v), 10 g/L tartaric acid adjusted to pH 3.4) was added to each sample. The addition was made in order to extract in approximately 15% ethanol. After the addition of nitrogen inert gas, the bottles' caps were sealed with paraffin film. The extraction took place for 40 h at 30 °C in a platform shaker. After the extraction step the samples were filtered through a kitchen sieve and the volume of extract recovered and analysed. Samples from both protocols were extracted in duplicate. Before analysis extracts were centrifuged at 3248*g* for 5 min in a 7366 Hermle centrifuge (Wehingen, Germany).

2.5. Spectrophotometric analysis of phenolic compounds

The high throughput format of the methyl cellulose precipitable tannin assay (MCP) reported by Mercurio, Dambergs, Herderich, and Smith (2007) from the original Sarneckis et al. (2006) method was used to estimate the total tannin content. The method uses the ability of the polymer to bind and precipitate tannins from solution. The tannin content is then calculated by comparing a control sample and a tannin precipitated sample. Initially, a methylcellulose (0.04% w/v; 1500 cP viscosity at 2%) and a saturated ammonium sulphate solution were prepared according to instructions (Mercurio et al., 2007). The treatment sample was prepared by adding 600 μL of MCP solution to 50 μL of wine, in a 2 mL microfuge tube. After 2–3 min, 400 μL of saturated ammonium sulphate solution and 950 μL distilled water were added. In the control samples the MCP solution was substituted by 600 μL distilled water. After 10 min both samples were centrifuged at 9279*g* for 5 min in an Eppendorf 5415D centrifuge (Hamburg, Germany). The absorbance was measured at 280 nm and the difference between the control and the treated samples was converted to epicatechin equivalents (mg/L) times the dilution factor (40). The MCP tannins assay was slightly modified for the grape extracts using the homogenate extraction protocol (Iland et al., 2000). In this case 200 μL of homogenate extract were used instead of 50 μL (as specified in the original protocol) and the water volume was adjusted accordingly (1100 μL) leading to a dilution factor of 10. The total tannin content in the grape extracts was calculated as follows:

$$\text{Tannin (mg/g)} = \text{Tannin extract (mg/L) x Volume extract (L) / Weight homogenate (g)} \quad (1)$$

Total anthocyanins were quantified with the method reported by Iland et al. (2000). Briefly, 100 μL of wine were diluted in 5 mL of hydrochloric acid 1 M. After dilution samples were kept in the dark for an hour, following the specification by Bindon et al. (2014). The absorbance at 520 nm was then recorded using a Multiskan GO Microplate Spectrophotometer (Thermo Fisher Scientific, Inc., Waltham, MA, USA). The anthocyanin content was calculated as malvidin-3-glucoside equivalents using the molar extinction coefficient (ε = 28.000 L/cm*mol) and the molecular weight (MW = 529 g/mol) of this compound times the dilution factor (DF = 51 for wines and wine-like extraction method and 20 for homogenate method). The calculations for wines (eq. (2)) and grapes (eq. (3)) were performed as follows:

$$\text{Anthocyanins (mg/L)} = \text{A520 nm x MW x DF} / \varepsilon \text{ x L} \quad (2)$$

$$\text{Anthocyanins (mg/g)} = \frac{\text{A520nm} \times \text{DF} \times \text{final extract (mL)} \times 1000}{500 \times 100 \times \text{homogenate weight (g)}} \quad (3)$$

All the absorbance values are referenced to the standard 1 cm pathlength (L). The Iland et al. (2000) methodology also allows for the calculation of the total phenolics index, which is calculated after recording the absorbance at 280 nm times the dilution factor as specified above. The protocol reported by Glories (1984) was used to determine the colour density. The absorbances at 420 nm, 520 nm and 620 nm were recorded after 50 μL of sample were pipetted into a UV-Visible Nunc F96 MicroWell plate (Nunc, Langenselbold, Germany). The colour density was obtained as the sum of the absorbance values of the three wavelengths referenced to 10 mm standard path length.

2.6. HPLC analysis of phenolic compounds

The method reported by Peng, Iland, Oberholster, Sefton, & Waters (2002) with some modification was used to quantify the phenolic compounds. The instrument used was an Agilent Technologies 1260 Infinity series (Agilent, Waldbronn, Germany) HPLC system with a PLRP-S polymeric reversed phased column (3 μm particle size, 100 Å pore size, 150 mm × 4.6 mm) at 35 °C. The gradient conditions were as follows: 0 min (5% solvent B), 73 (25% solvent B), 78 (50% solvent B), 86 (50% solvent B), 90 (5% solvent B). Acetonitrile and phosphoric acid in water at 1.5% were used as solvent A and B, respectively. The injection volume was 20 μL with an elution flow rate of 1 mL/min. A 15 min re-equilibration time between samples was established. The detection of the phenolic composition was done with a photodiode array detector. Gallic acid, monomeric and polymeric flavan-3-ols were detected at 280 nm. Phenolic acids and flavonols were identified at 320 nm and 360 nm, respectively. Finally, anthocyanins and polymeric pigments were detected at 520 nm. Calibration curves were built for gallic acid, catechin, caffeic acid, *p*-coumaric acid, quercetin-3-glucoside, quercetin and malvidin-3-glucoside. These calibration equations were used to quantify those compounds whose standards are not available. A chromatogram with peak identification and phenolic compounds identified can be observed in Supporting information S1.

2.7. UV-visible spectroscopy

Fermenting samples and wines were incubated for 1 h in the dark at room temperature after being diluted 51 times with HCl 1 M. Samples were scanned without temperature equilibration in a Multiskan GO Microplate Spectrophotometer (Thermo Fisher Scientific, Inc., Waltham, MA, USA) at 2 nm intervals over the wavelength range from 200 nm to 700 nm, with 1 M HCl as the reference blank.

2.8. Development and validation of the prediction models

Data analysis and model performance were evaluated using the PLS toolbox 8.2.1 available in MATLAB software version R2016b (Mathworks Inc., Natik, MA). The cross validation procedure was used to determine the optimal number of latent variables using the venetian blinds option with 10 data splits (10% of the data was left out for model calibration). The SIMPLS algorithm was used for the partial least squares regression. Forward interval variable selection (iPLS) was also investigated with the aim of discarding variables that might not be relevant for model building. A sequential and exhaustive search for individual or combinations of the best predictive variables was performed. Variable selection was used if the models were improved in terms of root mean square error of cross-validation (RMSECV). After the model optimization step the dataset was divided into calibration and validation sub sets using the Kennard-Stone (Kennard & Stone, 2016) and the onion methods at 50/50 and 66/33 calibration/validation ratios.

The percentage of variation explained by the model in the training (R^2cal) and validation set (R^2val), the fit of the observations to the model in both calibration (root mean standard error of cross validation (RMSECV)) and validation (root mean square error of prediction (RMSEP)) and the residual predictive deviation (RPD) in validation were reported. RMSECV provides the potential error of future predictions while RMSEP indicates the real error when predicting new samples and are expressed in the same units as the reference values. RPD values are provided in order to standardize the prediction accuracy (Fragoso et al., 2011). RPD is calculated as the standard deviation of the population divided by the root mean square error in prediction. High RPD values will be provided by large standard deviation and small prediction error. The higher the RPD the greater the ability of the model to accurately predict new samples.

Additionally, a slope and intercept test was evaluated to investigate any systematic error between predicted and reference data. The Deming approach (Linnet, 1993) was performed, consisting of a combined analysis on slope and intercept of the regression lines. The null hypothesis (Ho) corresponds to slope values equal to 1 and intercepts not different from 0 between predicted vs reference data at 95% confidence levels. The test measures differences between predicted and observed values to indicate if the differences are only due to random noise (Ho). This non-parametric regression approach is suitable for quantifications affected by non-negligible experimental error (Linnet, 1993). The predicted levels of phenolic compounds in the validation set were used to conduct the test. The test also does not impose that one of the methods is chosen as reference (UV-Vis spectroscopy or reference methods). Inter-class correlation coefficients (ICC) and standard "typical" error of measurement (SEM) were also calculated. ICC is a measurement of the consistency of the predicted values (reliability) (Weir, 2005) and ranges from 0 (non-reliable) to 1 (perfect reliability) at 95% confidence intervals. Moreover, an absolute measurement of reliability, in the same units as those reported by the reference methods, was provided by the standard error of measurement. It quantifies the precision of individual measurements i.e. the amount of error that can be assigned to the measurement error.

Finally, limit of detection (LOD) and limit of quantification (LOQ) of the PLS prediction models were also reported. LOD is considered to be a good estimator of the quality of a PLS models as it includes the concepts of the sensitivity and precision of an analytical measurement (Allegrini & Olivieri, 2014). The determination takes into account the latest IUPAC official recommendations and instead of a single value, an interval of LOD values is obtained (Allegrini & Olivieri, 2014). With this approach a characteristic LOD interval of the PLS regression model is provided. The LOQ was calculated as three times the LOD. The recommendations given by Olivieri (2015) and Williams, Dardenne, and Flinn (2017) were taken into account when reporting calibration results.

3. Results

3.1. Reference data

Basic statistics for the HPLC quantified phenolic compounds and for the four spectrophotometric parameters are reported in Table 1. The coefficient of variation (CV) explain the variability observed in the range of values for a specific phenolic compound. Coefficients

Table 1
Summary statistics of phenolic compounds and spectrophotometric measured parameters for the fermenting samples and wines.

Concentration (mg/L)	N	Average	Stdev	Min	Max	CV
Gallic acid	568	23,05	15	0,04	88,37	67
Catechin	566	35,31	19	0,98	186,31	54
B1	566	26,47	13	0,83	113,81	50
Polymeric phenols	569	753,05	426	52,72	2113,46	57
GRP	567	4,66	3,4	0,25	24,91	72
Caftaric acid	568	41,56	31	0,25	140,59	75
Caffeic acid	566	5,29	3,5	0,32	29,29	67
Coutaric acid	568	16,62	9,2	0,42	43,22	56
p-Coumaric acid	566	2,34	2,6	0,26	18,80	110
Quercetin-3-glucoside	568	46,26	35	0,27	155,09	75
Quercetin	561	6,99	5,4	0,45	32,78	77
Kaempherol	541	1,05	0,93	0,26	5,05	89
Delphinidin-3-glucoside	541	9,30	10,6	0,34	50,61	114
Cyanidin-3-glucoside	267	0,73	0,16	0,32	1,35	22
Petunidin-3-glucoside	546	13,11	11	0,45	46,26	86
Peonidin-3-glucoside	541	7,11	4,9	0,37	22,54	69
Malvidin-3-glucoside	563	104,88	75	0,56	288,71	72
Delphinidin-3-acetylglucoside	496	4,49	5,4	0,36	50,84	120
Cyanidin-3-acetylglucoside	337	2,81	1,3	0,47	7,58	46
Petunidin-3-acetylglucoside	521	4,31	3,8	0,30	15,48	88
Peonidin-3-acetylglucoside	544	4,85	3,7	0,36	12,72	76
Malvidin-3-acetylglucoside	560	34,31	28	0,59	108,59	80
Delphinidin-3-coumarylglucoside	427	2,04	1,4	0,30	5,95	67
Petunidin-3-coumarylglucoside	508	3,46	2,4	0,40	9,72	69
Peonidin-3-coumarylglucoside	544	3,93	3,7	0,29	15,66	94
Malvidin-3-coumarylglucoside	562	14,95	12	0,48	51,12	80
Polymeric pigments	566	31,63	20	1,90	119,74	62
Total phenols HPLC	569	1197.52	487	102.52	2510.85	41
MCP tannins	569	1456,87	808	56,85	3802,20	56
Anthocyanins	569	434,19	193	20,48	883,23	45
TPI	569	50,21	16	5,15	102,80	32
CD	569	17,65	7,4	2,28	56,97	42

N: number of samples; Stdev: standard deviation; Min: minimum; max: maximum; CV: coefficient of variation.

higher than 30% were always observed (with the exception of cyanidin-3-gluoside), which was interpreted as indicative of sufficient variability in the sample set for developing PLS calibration models (Aleixandre-Tudo et al., 2015). The concentrations reported here may be of interest as this is the most comprehensive survey of the range of the phenolic content in South African red wines. However, the data presented need to be considered indicative as the samples came from very diverse conditions such as different origin, cultivar, climate, ripening or winemaking conditions.

3.2. Correlation between spectrophotometric and HPLC determined phenolic levels

Interesting correlations were found between some spectrophotometric parameters and HPLC quantified phenolic compounds (Fig. 1). A strong positive correlation of 0.83 was observed between the MCP tannins assay values and polymeric phenols. The polymeric phenol peak is thought to be composed mainly of proanthocyanindins, but its use as an estimation of the total tannin content is currently not always accepted, as other polymeric phenols may also be included in the non-resolved elution peak (Kennedy & Waterhouse, 2000). Additionally, a strong positive correlation (0.81) was also observed for the TPI and the total HPLC quantified phenolics. Despite the limitations and simplicity of the TPI index this correlation indicated the value of this routine parameter to estimate the total phenolic content of wine.

3.3. Extraction of phenolic compounds during fermentation

Phenolic extraction takes place during the fermentation process while the solid parts of the berries are in contact with the must. The phenolic levels found in the 13 fermentations included in the study during approximately 25 days were averaged. Logarithmic regressions were fitted for the spectrophotometric parameters as well as for the HPLC quantified main phenolic families and can be observed in Fig. 2. The flavanols and proanthocyanidins group includes the compounds catechin, the polymer B1 and the polymeric phenols peak. Phenolic acids included the compounds quantified at 320 nm plus gallic acid, while flavonols include the compounds quantified at 360 nm. The anthocyanins group includes the glucosidated, acylated, *p*-cumaroylated anthocyanins and the polymeric pigments. Lastly, all the quantified compounds were added together to calculate the total phenolic content of a samples.

High coefficients of correlation ($R^2 > 0.80$) were always observed between the measured compounds and the fitted logarithmic equation during the fermentation process. The highest coefficients were observed for TPI, MCP tannins (spectrophotometer determinations) and the flavan-3-ols and proanthocyanidins and phenolic acids groups (HPLC quantified phenolics) ($R^2 > 0.9$). In addition to the good logarithmic correlations coefficients found, the extraction curves of colour density and the anthocyanin measurements showed a maximum around 15 days (more or less at pressing) with a subsequent steady decrease, which is in accordance to the results found in the literature (Ribéreau-Gayon, Glories, Maujean, & Dubourdieu, 2006) (Fig. 2).

3.4. UV-Vis spectroscopy prediction models for fermenting samples and wines

The statistics obtained from the different calibrations investigated in this study are shown in Table 2. Before model calibration the data was screened for outliers. Outliers are defined as samples

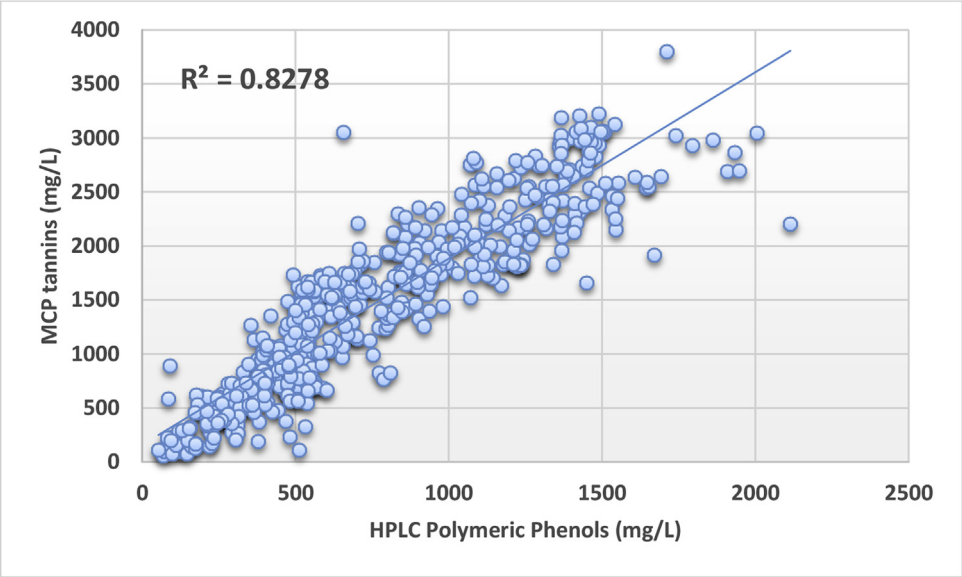

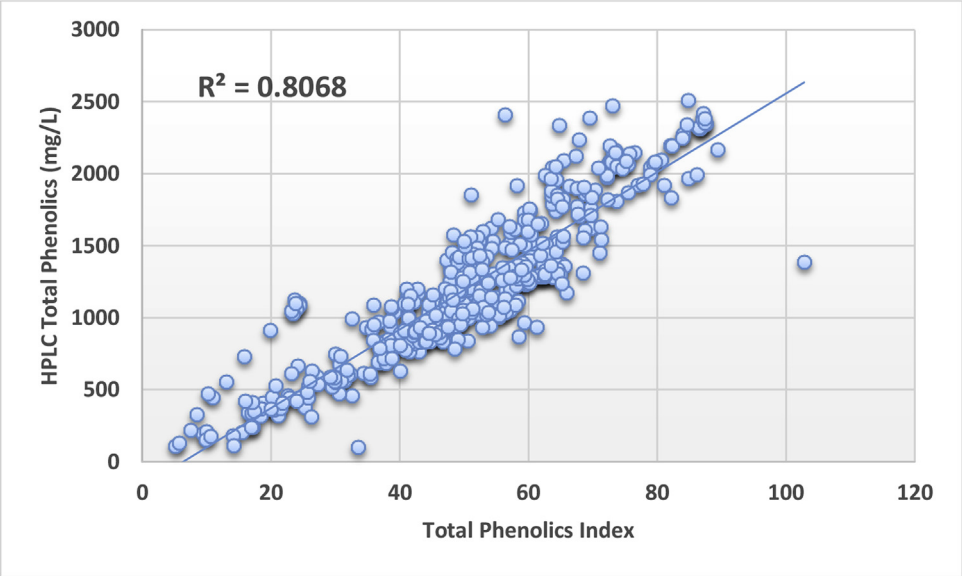

Fig. 1. Correlation between spectrophotometric and HPLC phenolic levels.

with abnormal spectral features or measured concentrations. Possible sources of error can be found during sampling, sample preparation, laboratory and/or analytical practices. Hotelling T^2 and leverage were also considered for outlier identification. Overall the number of outliers identified in the process of model calibration corresponded to 3.44% of the sample set. The number of samples included in the calibrations and the range of predicted concentrations, rank, calibration and validation statistics, bias, slope, SI test, ICC and SEM as well as $LOD_{min\text{-}max}$ and $LOQ_{min\text{-}max}$ are shown.

Spectral properties in the UV-VIS region of samples during fermentation and finished wines were collected in the 200–700 nm region are reported in supporting information S2. The main dominant features of the UV-VIS spectra corresponded to an absorption band at 280 nm, which corresponds to hydroxybenzoates, stilbenes, flavan-3-ols and to the UV absorption of the anthocyanins; 370 nm linked to the flavonols group and finally to a band around 520–540 nm that corresponds to the absorption part of the anthocyanins (Hong & Wrolstad, 1990). During the first days of the fermentation the most prominent change was observed at 520–540 nm with an increased absorption intensity, which can be ascribed to the anthocyanin extraction from grape skins into the wine. The same trend was observed for the absorption features at 280 nm and 370 nm, which were ascribed to the extraction of phenolic compounds that occurred during the red winemaking process. Moreover, towards the end of the fermentation and through aging the biggest changes were found as a decrease in the visible absorption band of the anthocyanins, together with the associated decrease of the UV absorption intensity of these compounds. This fact has been ascribed in the literature to different phenomena such as, polymeric pigment formation, oxidation, reabsorption in the skin and yeast cell wall and/or precipitation with tartaric salts, among others (Cozzolino, Parker, & Dambergs,

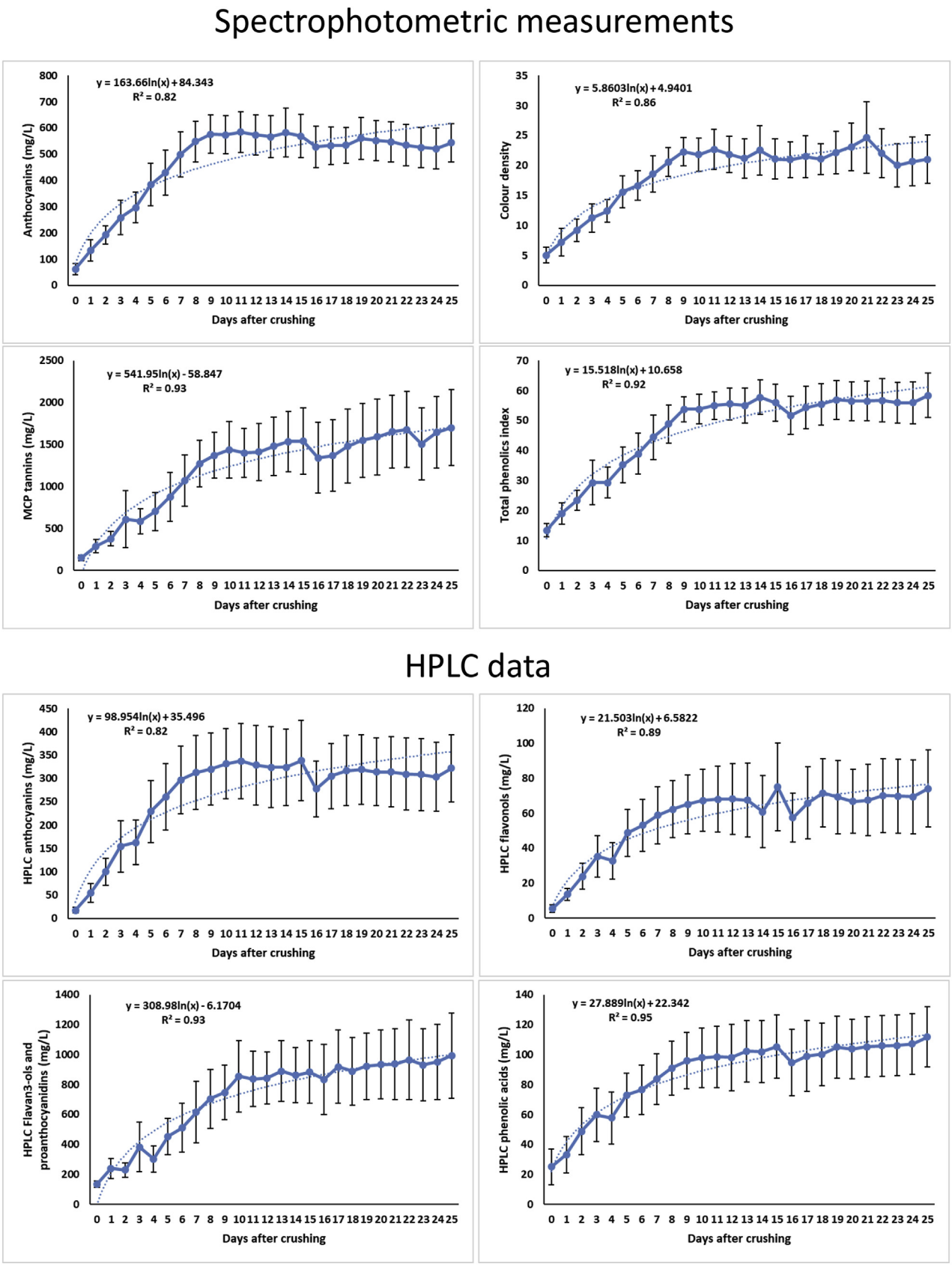

Fig. 2. Fermentation extraction curves with logarithmic equations and correlation coefficients. Average values and standard deviation of 13 fermentations.

Table 2
Summary statistics for the UV-VIS calibration and validation models built for the investigated phenolic measurements in fermenting samples and wines.

	N	Range	Rank	R^2cal	RMSECV	R^2val	RMSEP	RPD	Bias	Cal/Val	Slope	SI test	ICC	SEM	$LOD_{min-max}$	$LOQ_{min-max}$
Gallic acid	569	0.045–61.68	7	0.82	6.9	0.85	6	2.6	0.17	50/50	0.84	Ho rejected	0.92	4.3	1.3–1.4	3.9–4.09
Catechin	551	7.55–81.16	14	0.58	10	0.79	8	2.1	−1.18	66/33	0.89	Ho rejected	0.87	5.6	0.51–0.54	1.5–1.6
B1	540	0.83–51.8	14	0.75	6.4	0.75	5.7	2	0.26	66/33	0.82	Ho rejected	0.86	4.01	0.37–0.38	1.1–1.2
Polymeric phenols	551	71.55–2004.8	10	0.85	159	0.91	127	3.3	−6.52	50/50	0.93	Ho rejected	0.95	90	11–11	33–33
GRP	522	0.58–9.39	12	0.54	1.8	0.22	1.7	1.1	−0.02	66/33	0.25	Ho rejected	0.39	1.2	0.02–0.03	0.07–0.08
Caftaric acid	569	0.54–140.59	7	0.91	9.5	0.97	6.8	5.08	1.09	50/50	0.99	Ho rejected	0.98	4.5	0.09–0.1	0.28–0.3
Caffeic acid	515	0.48–9.28	12	0.64	1.7	0.73	1.6	1.9	−0.7	66/33	0.81	Ho rejected	0.82	1.1	0.18–0.2	0.55–0.59
Coutaric acid	543	0.66–38.92	5	0.83	3.5	0.9	3.2	2.9	−1	66/33	0.93	Ho rejected	0.93	2.2	0.1–0.1	0.29–0.29
p-Coumaric acid	550	0.26–11.29	8	0.56	1.4	0.7	1.3	1.8	−0.03	66/33	0.83	Ho rejected	0.8	0.91	0.01–0.02	0.04–0.05
Quercetin-3-glucoside	552	0.87–154.26	11	0.96	7.5	0.97	6.1	5.3	−2.17	50/50	0.99	Ho rejected	0.98	4.2	4.04–4.2	12–13
Quercetin	531	0.45–22.69	11	0.84	2.2	0.91	1.3	3.3	−0.31	50/50	0.87	Ho accepted	0.96	0.92	0.6–0.64	1.8–1.9
Kaempherol	510	0.3–5.05	8	0.77	0.45	0.89	0.31	2.8	−0.07	50/50	0.92	Ho rejected	0.93	0.21	0.09–0.1	0.26–0.3
Delphinidin-3-glucoside	540	0.84–50.61	10	0.8	5.01	0.87	4	2.8	0.39	66/33	0.88	Ho rejected	0.93	2.8	0.26–0.28	0.77–0.84
Cyanidin-3-glucoside	243	0.42–1	11	0.57	0.1	0.55	0.086	1.5	0.008	66/33	0.72	Ho rejected	0.71	0.06	0.02–0.03	0.06–0.09
Petunidin-3-glucoside	530	0.78–46.26	11	0.84	4.7	0.88	4.04	2.8	−1.51	66/33	0.94	Ho rejected	0.93	2.8	0.32–0.35	0.97–1.04
Peonidin-3-glucoside	527	0.37–22.23	5	0.59	2.9	0.81	2.3	2.1	0.22	66/33	0.91	Ho rejected	0.86	1.6	0.17–0.17	0.51–0.52
Malvidin-3-glucoside	524	4.3–288.71	11	0.84	28	0.88	26	2.7	2.71	66/33	0.83	Ho rejected	0.92	17	2.6–2.8	7.9–8.3
Delphinidin-3-acetylglucoside	460	0.41–16.13	8	0.85	1.7	0.88	1.4	2.9	0.045	66/33	0.89	Ho rejected	0.93	1	0.11–0.11	0.32–0.34
Cyanidin-3-acetylglucoside	310	0.52–544	6	0.79	0.54	0.79	0.49	2.1	0.13	66/33	0.8	Ho accepted	0.87	0.34	0.07–0.07	0.2–0.21
Petunidin-3-acetylglucoside	512	0.52–15.48	7	0.82	1.6	0.89	1.4	2.8	−0.23	50/50	0.95	Ho rejected	0.92	0.99	0.11–0.11	0.32–0.34
Peonidin-3-acetylglucoside	534	0.62–12.73	15	0.89	1.4	0.87	1.4	2.7	−0.16	66/33	0.89	Ho accepted	0.93	0.97	0.12–0.14	0.36–0.41
Malvidin-3-acetylglucoside	542	0.73–108.59	8	0.84	11	0.93	8.4	3.4	−0.49	66/33	0.91	Ho rejected	0.95	5.9	0.86–0.89	2.6–2.7
Delphinidin-3-coumarylglucoside	419	0.43–5.76	9	0.85	0.58	0.85	0.51	2.6	−0.09	50/50	0.87	Ho rejected	0.91	0.36	0.05–0.05	0.15–0.16
Petunidin-3-coumarylglucoside	505	0.47–8.98	13	0.86	1	0.84	0.92	2.5	−0.028	66/33	0.88	Ho accepted	0.92	0.65	0.09–0.1	0.26–0.3
Peonidin-3-coumarylglucoside	512	0.29–14.05	9	0.8	1.8	0.78	1.7	2.1	0.25	66/33	0.91	Ho rejected	0.88	1.2	0.1–0.1	0.29–0.31
Malvidin-3-coumarylglucoside	546	0.64–50.33	9	0.8	5.3	0.88	4.2	2.7	−0.18	66/33	0.9	Ho rejected	0.92	2.8	0.69–0.73	2.08–2.2
Polymeric pigments	531	1.97–83.1	14	0.81	7.9	0.86	5.8	2.6	−0.46	66/33	0.84	Ho rejected	0.92	4.04	0.48–0.52	1.4–1.6
MCP tannins	569	95.49–3101.55	6	0.92	239	0.93	209	3.7	−25.27	50/50	0.95	Ho rejected	0.96	148	188–191	563–574
Anthocyanins	569	40–883.23	4	0.99	15	0.99	14	13	0.58	50/50	0.99	Ho rejected	0.99	9.5	21–22	64–65
TPI	541	5.75–87.41	4	0.99	2.1	0.99	1.6	8.2	0.04	50/50	1	Ho accepted	0.99	1.2	2.2–3.3	6.6–6.9
CD	552	3.4–39.47	7	0.85	2.8	0.87	2.6	2.6	0.04	50/50	0.91	Ho rejected	0.91	1.8	3.05–3.3	9.2–10.1

N: number of samples; R^2cal: coefficient of correlation in calibration; RMSECV: root mean standard error in cross validation; R^2val: coefficient of correlation in validation; RPD: residual predictive deviation; Cal/Val: calibration/validation ratio; SI test: slope and intercept test; ICC: interclass correlation coefficients; SEM: standard error of measurement; $LOD_{min-max}$: maximum and minimum limit of detection; $LOQ_{min-max}$: maximum and minimum limit of quantification.

2006; He et al., 2012b, 2012a; Sanna et al., 2014).

On a general basis, the loading analysis of the first latent variable (explaining around or more than 90% of the variance) presented the same features as the UV-Visible spectra of the samples. The reason might be due to the fact that the UV-Visible spectra of the wines is dominated to a large extent by phenolic compounds, while the most abundant components in the sample matrices do not show strong spectral features in this specific region of the electromagnetic spectrum.

As can be observed in Table 3, prediction models with RPD values higher than 2.5 were obtained for the majority of the compounds and parameters under study. Calibrations with RPD's higher than 2.5 can be used for phenolic prediction purposes, as reported by several authors (Aleixandre-Tudo et al., 2015; Cozzolino et al., 2004; Dambergs et al., 2012). Additionally, prediction models with RPD 1.5–2.5 may be used for screening purposes. As is evident from the results in Table 3, two thirds of the compounds and parameters investigated could be accurately quantified using the UV-VIS spectra information. The best models were obtained for polymeric phenols, caftaric acid, quercetin-3-glucoside, quercetin, malvidin-3-acetylglucoside, MCP tannins, anthocyanins and TPI with RPD values higher than 3. MCP tannins models with similar accuracy, built only with a limited number of wavelengths in the UV region were also reported by other authors (Aleixandre-Tudo et al., 2015; Dambergs et al., 2012). The calibration for polymeric pigments also showed an RPD higher than 2.5. A strong correlation between these compounds and the SO_2 resistant pigments parameter obtained from the modified Somers method (Mercurio et al., 2007) has been reported in the literature (Aleixandre-Tudo et al., 2017). The compounds catechin, peonidin-3-glucoside, cyanidin-3-acetylglucoside and peonidin-3-cumaryglucoside showed models with RPD values higher than two and might be thus also considered for sample screening. Moreover, approximately one third of the calibrations were externally validated with calibration/validation ratios at 50/50, which in most cases coincided with the models that showed the highest acfcuracy. Keeping the calibration/validation ratio as similar as possible is an indication of model robustness as calibrations have been tested against a larger number of samples. However, calibration/validation ratios of 66/33 are widely accepted and are not considered detrimental in model evaluation (Williams et al., 2017). On the other hand, the slope values smaller than 1, for some models (Tables 2 and 4), may be an indication of non-linearity at higher concentrations. However, the ranges of phenolic levels reported in this study were accurately modelled using a linear regression

Table 3
Summary statistics of grape phenolic parameters using the homogenate and the wine like extraction protocols.

	N	Average	Stdev	min	max	CV
HOMOGENATE						
MCP (mg/g)	260	3.14	0.71	1.07	5.49	23
Anthocyanins (mg/g)	260	1.11	0.40	0.18	2.73	36
TPI	260	12.80	2.6	4.84	22.91	20
CD	260	10.92	3.8	2.32	25.43	35
WINE LIKE						
MCP (mg/g)	260	1.12	0.46	0.11	2.74	41
Anthocyanins (mg/g)	260	0.36	0.17	0.05	1.00	47
TPI	260	42.78	15	15.03	107.30	35
CD	260	30.33	17	3.83	89.31	56

N: number of samples; Stdev: standard deviation; Min: minimum; max: maximum; CV: coefficient of variation.

Table 4
Summary statistics for the UV-VIS calibration and validation models built for the investigated phenolic parameters in grape samples (homogenate and wine-like extraction).

	N	Range	Rank	R^2cal	RMSECV	R^2val	RMSEP	RPD	Bias	Cal/Val	Slope	SI test	ICC	SEM	$LOD_{min-max}$	$LOQ_{min-max}$
HOMOGENATE																
MCP tannins (mg/g)	259	2.17–4.96	7	0.91	0.27	0.85	0.22	2.6	−0.01	66/33	0.86	Ho rejected	0.9	0.19	0.41–0.44	1.2–1.3
Anthocyanins (mg/g)	259	0.28–1.69	2	0.99	0.04	0.98	0.034	7.3	0.001	50/50	0.99	Ho accepted	0.98	0.034	0.04–0.04	0.12–0.12
TPI	260	8.83–17.52	4	0.99	0.17	0.99	0.17	10.6	0.03	50/50	0.99	Ho rejected	0.99	0.12	0.58–0.6	1.8–1.8
CD	260	2.37–17.68	2	0.93	1.2	0.94	0.72	3.8	−0.002	50/50	0.95	Ho accepted	0.96	0.48	2.2–2.2	6.6–6.6
WINE-LIKE																
MCP tannins (mg/g)	258	0.19–2.74	4	0.94	0.11	0.94	0.12	3.9	0.004	50/50	0.97	Ho accepted	0.93	0.13	0.14–0.15	0.43–0.46
Anthocyanins (mg/g)	260	0.09–1	3	0.98	0.02	0.98	0.03	6.1	−0.001	50/50	1.01	Ho rejected	0.99	0.022	0.01–0.01	0.02–0.03
TPI	260	18.63–107.3	3	0.99	0.32	0.99	0.42	39	0.04	50/50	1	Ho accepted	1	0.3	1.9–2.08	5.6–6.2
CD	251	7.69–88.25	8	0.74	8.5	0.87	6.2	2.7	1.11	50/50	0.91	Ho rejected	0.93	4.3	5.2–6	16–18

N: number of samples; R^2cal: coefficient of correlation in calibration; RMSECV: root mean standard error in cross validation; R^2val: coefficient of correlation in validation; RPD: residual predictive deviation; Cal/Val: calibration/validation ratio; SI test: slope and intercept test; ICC: interclass correlation coefficients; SEM: standard error of measurement; $LOD_{min-max}$: maximum and minimum limit of detection; $LOQ_{min-max}$: maximum and minimum limit of quantification.

procedure, as can be observed throughout the different statistics reported.

The null hypothesis (Ho) was rejected in most of the cases as can be observed in Table 3, indicating slopes different from 1 and intercepts not containing 0 at 95% confidence interval. Only the compounds quercetin, cyanidin-3-acetylglucoside and peonidin-3-acetylglucoside, petunidin-3-coumarylglucoside and the parameter total phenolic index confirmed the null hypothesis (Ho accepted). The results showed a systematic error between the values predicted with the calibrations and the reference data, however the joint slope and intercept test (SI) test does not provide information about the magnitude of the error. It is possible that large differences between the observed vs. predicted values existed despite the null hypothesis still being confirmed. With the aim of investigating the reliability of the predictions ICC and SEM were also investigated. Twenty-two out of 31 calibrations presented ICC values higher than 0.9 indicating that a high proportion of the differences are part of the observed vs. predicted values. Another group of compounds showed ICC >0.85 including catechin, B1, peonidin-3-glucoside, cyanidin-3-acetylglucoside (Ho accepted) and peonidin-3-coumarylglucoside. SEM values, which provide the amount of error that can be assigned to the measurement error, were found to be at all cases lower than RMSEP.

The limit of detection (LOD) of a PLS models is a good indication of the accuracy of a calibration and provides the lowest quantity of a substance that can be distinguished from the absence of that substance (Allegrini & Olivieri, 2014). The calculation of the LOD requires the estimation of the optimum number of latent variables in the cross validated model as well as the uncertainty in both signal and calibration concentrations. The uncertainty in the UV-VIS signal was calculated as 0.007 AU and obtained by measuring the UV-VIS spectra (200–700 nm) of the same wine samples eight times. The uncertainties in the reference methods were obtained in a similar manner with the sample analysed eight times for HPLC phenolic compounds as well as for the other reported parameters. For the HPLC phenolics those compounds whose standards were available were used as references for the determination of the uncertainty in calibration (e.g. the uncertainty of catechin was used for B1 and polymeric phenols LODs determination). Standard deviation values in percentage of 1.74%, 0.17%, 0.44%, 0.74%, 2.6% were obtained for gallic acid, caftaric acid, catechin, malvidin-3-glucoside and quercetin-3-glucoside, respectively. Moreover, the uncertainty of the phenolic parameters was as follow: 3.88%, 1.5%, 1.3%, 5.1% for MCP tannins, anthocyanins, TPI and CD, respectively. The calculation of the uncertainty for MCP tannins was slightly different as two sets of eight replicates of the same samples were analysed. The uncertainty was calculated as the average of the two sets. This was done with the aim of maintaining the procedure followed for the determination of the MCP tannin content. As the MCP protocol requires 10 min of waiting time plus 5 min of centrifugation a new set of eight samples is started while waiting. By doing this the analytical time is substantially reduced and a large number of samples can thus be analysed.

The majority of the calibrations showed LOD ranges lower than the lowest concentration predicted by the calibrations (Table 3). Only for gallic acid, quercetin-3-glucoside, quercetin, malvidin-3-acetylglucoside, malvidin-3-coumarylglucoside and MCP tannins the lowest predicted concentration was below the $LOD_{min-max}$ values. When investigating the LOQ almost half of the calibrations showed LOQ ranges lower than the lowest predicted concentration. The results observed here have thus to be taken into consideration especially during the very early stages of fermentation when the predicted values can be found below the LOQ or LOD ranges.

3.5. UV-Vis spectroscopy prediction models for grape extracts

Prediction models for MCP tannins (mg/g), anthocyanins (mg/g), TPI and CD were constructed for a set of 130 grape samples spanning a wide range of cultivars, origins and levels of phenolic compounds. Two extraction protocols, namely homogenate (Iland et al., 2000) and wine-like (Bindon et al., 2014) methods, were investigated and a summary of statistics is reported in Table 3. Spectral features collected with both extraction methods are represented in supporting information S3 and S4. Wine-like MCP tannins and anthocyanin values were in accordance to those reported by Bindon et al. (2014) for Australian Cabernet Sauvignon and Shiraz samples. The minimum levels reported in this study were lower because of the inclusion of cultivars such as Cinsault or Red Muscadel that are generally characterized as low phenolic containing cultivars. The phenolic levels observed here for the homogenate extraction were also in accordance to those reported elsewhere (Bindon et al., 2014). Such a large set of data is presented here for the first time and can thus be a good indication of the levels of phenolic compounds in South African red wine cultivars. In addition to this, a large range of concentrations and high coefficients of variation were observed for the investigated parameters and for both extraction procedures (Table 3).

The ranges of predicted concentrations, calibration and validation statistics, SI test, ICC and SEM and LOD and LOQ values are reported in Table 4. Table 4 shows accurate models (RPD > 2.5) for MCP tannins (mg/g), anthocyanins (mg/g), TPI and CD parameters for grape extracts obtained with the homogenate method. Calibration/validation ratios were kept at 50/50, except for the MCP tannin model. With regards to the null hypothesis, it was accepted for the anthocyanins and CD calibrations showing thus these models increased robustness, as the slope is equal to 1 and the

intercept is placed at 0, with 95% confidence intervals. Moreover, ICC values were always equal or higher than 0.9 with also low SEM values reported. Additionally, LOD ranges were also below the lowest predicted value. However, when LOQ was investigated the CD model showed a range ($LOQ_{min-max} = 6.6–6.64$) higher than the lowest predicted concentration indicating lower precision of the CD model. For the other three parameters LOQ was also lower than the lowest predicted concentration. Accurate prediction models were also observed for the wine like extracted grape phenolics (Table 4). In this case ratios were always kept at 50/50 calibration/validation. Contrarily to what was observed previously the null hypothesis was confirmed (Ho accepted) for the MCP tannins and TPI models with ICC values equal or higher than 0.93 with also appropriate measurement errors. Moreover, LODs were always lower than the lowest predicted sample. On the other hand, LOQs were higher than the lowest predicted concentration for the MCP tannins and CD models fact that was not observed for the anthocyanins and TPI models.

4. Discussion

This research study has demonstrated that UV-Vis spectroscopy is also a valid alternative for the phenolic profiling of samples during the fermentation and in finished wines. In combination with the main phenolic parameters (namely, tannins, anthocyanins, TPI and CD) a detailed phenolic profiling of the samples during the winemaking process could thus be achieved by using the information contained in the UV-Vis spectra of the samples. Currently, only advanced chromatographic methods, such as HPLC, are normally required. Accurate RPD values were obtained for the majority of the calibrations. A detailed anthocyanin characterization together with prediction of the main phenolic acids and flavonols is now feasible, using only UV-Visible spectroscopy.

The investigation of models to predict some phenolic parameters for grape samples, with the use of two different extraction protocols were also found to be successful. The wine-like extraction method, which is a longer procedure, provides a better estimation of the phenolic levels that will be later found in wine (specifically for tannins) (Bindon et al., 2014). The homogenate extraction is also a valid alternative and a widely used method being these the main reason of its inclusion in this study.

Additionally, the models have been tested to a large extent with the inclusion of other statistical estimators, aiming to provide further understanding on the accuracy and robustness of the prediction calibrations. From the SI test results, the null hypothesis was in most cases rejected which indicated the slope being different from 1 (the calibrations might provide larger errors towards the extremes) and intercepts not place at 0 (possibly leading to a systematic over- or under-estimation) at 95% confidence intervals. For every comparison (observed vs predicted) a further investigation into the nature of the error was achieved by evaluating the Bland and Altman plots (data not shown). The plot provides an overview of the validation residuals against the average observed/predicted. The nature of the systematic error if any can thus be identified. The validation samples generally appeared scattered throughout the plot indicating absence of a specific type of error for the calibrations under study. However, ICC showed values almost always higher than 0.9 with low SEM indicating reliability in the predictions. Moreover, LOD and LOQ of the PLS calibrations of phenolic compounds in grapes, fermenting samples and wines are reported here for the first time. The calculation of these two estimators indicated that in most cases LODs and LOQs were lower than the lowest predicted concentration. However, for some other calibrations attention should be paid during the first days of the fermentation or in lower phenolic containing grape and wine samples as the levels of some phenolic compounds and parameters are above the LOD or the LOQ ranges provided. This is for example the case for the MCP tannins levels and CD. Looking at Fig. 2 and Table 2 the MCP tannin predictions are only higher than the LOQ after more or less three days from the beginning of the fermentation (approximately at 600 mg/L). On the contrary anthocyanins and TPI levels can be predicted from day 0. With regards to colour density only predictions obtained after three days (CD = 10) of the fermentation start will be above the LOQ. The higher uncertainty observed for the MCP tannins and CD reference methods seems to play a role on the LOD and LOQ values for these calibrations. The calculation of the LOD and LOQ parameters includes the vector of PLS regression coefficients, the calibration concentrations, the rank and the uncertainties in both signal (UV-Visible spectroscopy) and reference methods. Model performance as well as accuracy in spectral collection and reference data generation are thus taken into account. The LOD and LOQ parameters are therefore a measurements of the overall accuracy of a PLS models (all the components of a PLS calibration are included) providing therefore an important alternative estimator to evaluate the quality of a PLS calibration.

The implementation of process control in wine production is currently demanding new analytical strategies. The incorporation of process analytical technologies (PAT) during the winemaking production chain will ensure the required quality standards. Analytical technologies include a variety of resources that provide a better understanding of product properties. Early identification of product quality deviations is one of the main benefits of the inclusion of PAT into the production process (Rathore, Bhushan, & Hadpe, 2011). Phenolic compounds are key components in red wine production as they contribute to a large extent to the organoleptic properties of the final product. The possibility of obtaining information related to phenolic compounds during the fermentation and aging processes of red wines in a fast, simple and accurate manner becomes therefore essential.

The use of spectroscopy with chemometrics appears as a potential technique to provide the phenolic information. Infrared spectroscopy has been reported as a technique suitable for this purpose, with a potential extension to on-line and in-line process control and monitoring (Aleixandre-Tudo et al., 2017; Dambergs et al., 2015; Daniel, 2015; Ricci et al., 2013). However, the acquisition of infrared instruments is not always possible for medium and small size wineries with limited resources. UV-Vis spectroscopy, which is a more affordable technology, could thus be an alternative. Spectra acquisition in UV-Vis spectroscopy, requires a samples preparation step where the samples need to be diluted with hydrochloric acid to avoid saturation of the detector (Dambergs et al., 2012). This additional step limits the use of this technique to on-line applications but the economic benefits might justify its selection. Moreover, recent advances in instrumentation development may provide in the near future UV-Vis spectrophotometers with detectors capable to handle saturation conditions. Finally, as the UV-Vis detectors often provide different responses, additional effort should be made in terms of instrument to instrument calibrations transfer. When samples are intended for prediction in a new instrument a calibration transfer method should be considered. The application of slope and bias correction, among other calibration transfer methods, has been proposed (Dambergs et al., 2012) and may thus be considered.

5. Conclusions

The results observed in this research study found UV-Visible spectroscopy as a suitable technique for phenolic monitoring during the fermentation process as well as in finished wines. Additionally, calibrations for some of the most common phenolic

parameters were also obtained for grape phenolic extracts, following two different extraction protocols. The inclusion of SI test and LOD and LOQ calculations extended on the evaluation of model performance, in terms of robustness and accuracy. UV-Vis technology can thus be considered a valid option for process control and monitoring of the phenolic behaviour and evolution throughout the winemaking process.

Acknowledgments

The authors gratefully acknowledge the Valid program of the Conselleria de Educacio, Cultura i Esport (APOSTD 2014/035) (Generalitat Valencia), the National Research Foundation (NRF Free-standing postdoctoral fellowship) (grant number 85242) and Winetech South Africa (WdT 13/01 and WdT 15/02) for financial support during the postdoctoral research collaboration between Stellenbosch University and Polytechnic University of Valencia.

Appendix A. Supplementary data

Supplementary data related to this article can be found at https://doi.org/10.1016/j.foodcont.2017.09.014.

References

Aleixandre-Tudo, J. L., Buica, A., Nieuwoudt, H., Aleixandre, J. L., & du Toit, W. (2017). Spectrophotometric analysis of phenolic compounds in grapes and wines. *Journal of Agricultural and Food Chemistry, 65*(20), 4009–4026.

Aleixandre-Tudo, J. L., Nieuwoudt, H., Aleixandre, J. L., & Du Toit, W. J. (2015). Robust ultraviolet-visible (UV-vis) partial least-squares (PLS) models for tannin quantification in red wine. *Journal of Agricultural and Food Chemistry, 63*(4), 1088–1098.

Aleixandre, J. L., Aleixandre-Tudó, J. L., Bolaños-Pizarro, M., & Aleixandre-Benavent, R. (2013). Mapping the scientific research on wine and health (2001 – 2011). *Journal of Agricultural and Food Chemistry, 61*, 11871–11880.

Allegrini, F., & Olivieri, A. C. (2014). IUPAC-consistent approach to the limit of detection in partial least- squares calibration. *Analytical Chemistry, 86*, 7858–7866.

Arranz, S., Chiva-blanch, G., Valderas-martínez, P., Medina-remón, A., Lamuela-raventós, R. M., & Estruch, R. (2012). *Wine, beer, alcohol and polyphenols on cardiovascular disease and cancer, (Cvd)*.

Beaver, C. W., & Harbertson, J. F. (2016). Comparison of multivariate regression methods for the analysis of phenolics in wine made from two vitis vinifera cultivars. *American Journal of Enology and Viticulture, 67*(1), 56–64.

Bindon, K. A., Kassara, S., Cynkar, W. U., Robinson, E. M. C., Scrimgeour, N., & Smith, P. A. (2014). Comparison of extraction protocols to determine differences in wine-extractable tannin and anthocyanin in Vitis vinifera L. cv. Shiraz and Cabernet Sauvignon grapes. *Journal of Agricultural and Food Chemistry, 62*, 4558–5457.

Boido, E., Alcalde-Eon, C., & Carrau, F. (2006). Aging effect on the pigment composition and color of Vitis vinifera L. cv. Tannat wines. Contribution of the main pigment families to wine color. *Journal of Agricultural and Food Chemistry, 54*, 6692–6704.

Casas, R., Chiva-blanch, G., Urpi-sarda, M., Llorach, R., Rotches-ribalta, M., Guille, M., … Estruch, R. (2012). Differential effects of polyphenols and alcohol of red wine on the expression of adhesion molecules and inflammatory cytokines related to atherosclerosis: A randomized clinical trial. *American Journal of Clinic Nutrition, 95*, 326–334.

Chen, S., Zhang, F., Ning, J., Liu, X., Zhang, Z., & Yang, S. (2015). Predicting the anthocyanin content of wine grapes by NIR hyperspectral imaging. *Food Chemistry, 172*, 788–793.

Cheynier, V., Dueñas-Paton, M., Salas, E., Maury, C., Souquet, J. M., Sarni-Manchado, P., et al. (2006). Structure and properties of wine pigments and tannins. *American Journal of Enology and Viticulture, 57*(3), 298–305.

Chiva-blanch, G., Arranz, S., Lamuela-raventos, R. M., & Estruch, R. (2013). Effects of wine, alcohol and polyphenols on cardiovascular disease risk factors. *Evidences from Human Studies, 48*(3), 270–277.

Cozzolino, D. (2015). The role of visible and infrared spectroscopy combined with chemometrics to measure phenolic compounds in grape and wine samples. *Molecules, 20*, 726–737.

Cozzolino, D., Kwiatkowski, M. J., Parker, M., Cynkar, W. U., Dambergs, R. G., Gishen, M., et al. (2004). Prediction of phenolic compounds in red wine fermentations by visible and near infrared spectroscopy. *Analytica Chimica Acta, 513*(1), 73–80.

Cozzolino, D., Parker, M., & Dambergs, R. (2006). Chemometrics and Visible-Near Infrared spectroscopic monitoring of red wine fermentation in a pilot scale. *Biotechnology and Bioingeneering, 95*(6), 1017–1101.

Dambergs, R., Gishen, M., & Cozzolino, D. (2015). A review of the state of the art, limitations, and perspectives of infrared spectroscopy for the analysis of wine grapes, must, and grapevine tissue. *Applied Spectroscopy Reviews, 50*(3), 261–278.

Dambergs, R. G., Mercurio, M. D., Kassara, S., Cozzolino, D., & Smith, P. A. (2012). Rapid measurement of methyl cellulose precipitable tannins using ultraviolet spectroscopy with chemometrics: Application to red wine and inter-laboratory calibration transfer. *Applied Spectroscopy, 66*(6), 656–664.

Daniel, C. (2015). The role of visible and infrared spectroscopy combined with chemometrics to measure phenolic compounds in grape and wine samples. *Molecules, 20*(1), 726–737.

Fernandes, A. M., Oliveira, P., Moura, J. P., Oliveira, A. A., Falco, V., Correia, M. J., et al. (2011). Determination of anthocyanin concentration in whole grape skins using hyperspectral imaging and adaptive boosting neural networks. *Journal of Food Engineering, 105*(2), 216–226.

Ferrer-Gallego, R., Hernández-Hierro, J. M., Rivas-Gonzalo, J. C., & Escribano-Bailón, M. T. (2011). Determination of phenolic compounds of grape skins during ripening by NIR spectroscopy. *LWT - Food Science and Technology, 44*(4), 847–853.

Fragoso, S., Aceña, L., Guasch, J., Busto, O., & Mestres, M. (2011). Application of FT-MIR spectroscopy for fast control of red grape phenolic ripening. *Journal of Agricultural and Food Chemistry, 59*(6), 2175–2183.

Fulcrand, H., Dueñas, M., Salas, E., & Cheynier, V. (2006). Phenolic reactions during winemaking and aging. *American Journal of Enology and Viticulture, 57*(3), 289–297.

García-Jares, C., & Medina, B. (1995). Prediction of some physico-chemical parameters in red wines from ultraviolet-visible spectra using a partial least-squares model in latent variables. *Analyst, 120*(7), 1891–1896.

Garrido, J., & Borges, F. (2013). Wine and grape polyphenols - a chemical perspective. *Food Research International, 54*(2), 1844–1858.

Gishen, M., Dambergs, R. G., & Cozzolino, D. (2005). Grape and wine analysis - enhancing the power of spectroscopy with chemometrics. *Australian Journal Of Grape And Wine Research, 11*(3), 296–305.

Glories, Y. (1984). La couleur des vins rouges, 2eme partie. *Connaissance de La Vigne et Du Vin, 18*, 253–271.

Harbertson, J. F., Mireles, M., & Yu, Y. (2015). Improvement of BSA tannin precipitation assay by reformulation of resuspension buffer. *American Journal of Enology and Viticulture, 66*(1), 95–99.

Harbertson, J. F., Picciotto, E. A., & Adams, D. O. (2003). Measurement of polymeric pigments in grape berry extracts and wines using a protein precipitation assay combined with bisulfite bleaching. *American Journal of Enology and Viticulture, 54*(4), 301–306.

Harbertson, J. F., & Spayd, S. (2006). Measuring phenolics in the winery. *American Journal of Enology and Viticulture, 57*, 280–288.

Hassane, E., Gierschner, J., Duroux, J., & Trouillas, P. (2012). UV/visible spectra of natural polyphenols: A time-dependent density functional theory study. *Food Chemistry, 131*(1), 79–89.

He, F., Liang, N. N., Mu, L., Pan, Q. H., Wang, J., Reeves, M. J., et al. (2012a). Anthocyanins and their variation in red wines I. Monomeric anthocyanins and their color expression. *Molecules, 17*(2), 1571–1601.

He, F., Liang, N. N., Mu, L., Pan, Q. H., Wang, J., Reeves, M. J., et al. (2012b). Anthocyanins and their variation in red wines II. Anthocyanin derived pigments and their color evolution. *Molecules, 17*(2), 1483–1519.

Hong, V., & Wrolstad, R. E. (1990). Characterization of anthocyanin-containing colorants and fruit juices by HPLC/photodiode array detection. *Journal Of Agricultural And Food Chemistry, 38*(3), 698–708.

Iland, P., Ewart, A., Sitters, J., Markides, A., & Bruer, N. (2000). *Techniques for chemical analysis and quality monitoring during winemaking* (1st ed., pp. 1–111). Campbelltown, South Australia: Patrick Iland Wine Promotions.

Jensen, J. S., Werge, H. H. M., Egebo, M., & Meyer, A. S. (2008). Effect of wine dilution on the reliability of tannin analysis by protein precipitation. *American Journal of Enology and Viticulture, 59*(1), 103–105.

Kennard, A. R. W., & Stone, L. A. (2016). American society for quality computer aided design of experiments american society for quality stable URL. *Computer Aided Design of Experiments, 11*(1), 137–148.

Kennedy, J. A., & Waterhouse, A. L. (2000). Analysis of pigmented high-molecular-mass grape phenolics using ion- pair, normal-phase high-performance liquid chromatography. *Journal of Chromatography A, 866*(1), 25–34.

Linnet, K. (1993). Evaluation of regression procedures for methods comparison studies. *Clinical Chemistry, 39*(3), 424–432.

Lorrain, B., Ky, I., Pechamat, L., & Teissedre, P. L. (2013). Evolution of analysis of polyhenols from grapes, wines, and extracts. *Molecules, 18*(1), 1076–1100.

Mercurio, M. D., Dambergs, R. G., Herderich, M. J., & Smith, P. A. (2007). High throughput analysis of red wine and grape phenolics - adaptation and validation of methyl cellulose precipitable tannin assay and modified somers color assay to a rapid 96 well plate format. *Journal of Agricultural and Food Chemistry, 55*(12), 4651–4657.

Olivieri, A. C. (2015). Practical guidelines for reporting results in single- and multi-component analytical calibration: A tutorial. *Analytica Chimica Acta, 868*, 10–22.

Peng, Z., Iland, P. G., Oberholster, A., Sefton, M. A., & Waters, E. J. (2002). Analysis of pigmented polymers in red wine by reverse phase HPLC. *Australian Journal of Grape and Wine Research, 8*(1), 70–75.

Rathore, A. S., Bhushan, N., & Hadpe, S. (2011). Chemometrics applications in biotech processes: A review. *Biotechnology Progress, 27*(2), 307–315.

Ribéreau-Gayon, P., Glories, Y., Maujean, A., & Dubourdieu, D. (2006). Handbook of

Enology: The microbiology of wine and vinifications. *Handbook of Enology, 2*.
Ricci, A., Parpiniello, G., Laghi, L., Lambri, M., & Versari, A. (2013). Application of infrared spectroscopy to grape and wine analysis. In D. Cozzolino (Ed.), *Chapter of the book: "Infrared spectroscopy: Theory, developments and applications"* (pp. 17–41). Hauppauge, NY: Nova Science Publishers, Inc., ISBN 978-1-62948-521-8 (2013).
Sacchi, K. L., Bisson, L. F., & Adams, D. O. (2005). A review of the effect of wine-making techniques on phenolic extraction in red wines. *American Journal of Enology and Viticulture, 56*(3), 197–206.
Sanna, R., Piras, C., Marincola, F. C., Lecca, V., Maurichi, S., & Scano, P. (2014). Multivariate statistical analysis of the UV-vis profiles of wine polyphenolic extracts during vinification. *Journal of Agricultural Science, 6*(12), 152–162.
Sarneckis, C. J., Dambergs, R. G., Jones, P., Mercurio, M., Herderich, M. J., & Smith, P. A. (2006). Quantification of condensed tannins by precipitation with methyl cellulose: Development and validation of an optimised tool for grape and wine analysis. *Australian Journal of Grape and Wine Research, 12*(1), 39–49.
Skogerson, K., Downey, M., Mazza, M., & Boulton, R. (2007). Rapid determination of phenolic components in red wines from UV-visible spectra and the method of partial least squares. *American Journal of Enology and Viticulture, 58*(3), 318–325.
Smith, P. A., Mcrae, J. M., & Bindon, K. A. (2015). Impact of winemaking practices on the concentration and composition of tannins in red wine. *Australian Journal of Grape and Wine Research, 21*, 601–614.
Sun, B., Leandro, C., Ricardo da Silva, J. M., & Spranger, I. (1998). Separation of grape and wine proanthocyanidins according to their degree of polymerization. *Journal of Agricultural and Food Chemistry, 46*(4), 1390–1396.
Sun, A. Y., Wang, Q., Simonyi, A., & Sun, G. Y. (2010). *Resveratrol as a therapeutic agent for neurodegenerative diseases*.
Teixeira, A., Eiras-Dias, J., Castellarin, S. D., & Gerós, H. (2013). Berry phenolics of grapevine under challenging environments. *International Journal of Molecular Sciences, 14*(9), 18711–18739.
du Toit, W. J., & Visagie, M. (2012). Correlations between south african red grape and wine colour and phenolic composition: Comparing the glories, iland and bovine serum albumin tannin precipitation methods. *South African Journal of Enology and Viticulture, 33*(1), 33–41.
Versari, A., Parpinello, G. P., & Laghi, L. (2012). Application of infrared spectroscopy for the prediction of color components of red wines. *Spectroscopy (Duluth, MN, United States), 27*(2), 36–47.
Weir, J. P. (2005). Quatifying test-retest reliability using the intraclass correlation coefficient and the SEM. *Journal of Strength and Conditioning Research, 19*(1), 231–240. ht.
Williams, P., Dardenne, P., & Flinn, P. (2017). Tutorial: Items to be included in a report on a near infrared spectroscopy project. *Journal of Near Infrared Spectroscopy, 25*(2), 85–90.